

PHYSICAL METALLURGY
AND HEAT TREATMENT

Influence of Ultrafine-Grained Structure on the Kinetics and Fatigue Failure Mechanism of VT6 Titanium Alloy

G. V. Klevtsov^{a, *}, R. Z. Valiev^{b, **}, I. P. Semenova^{b, ***}, N. A. Klevtsova^{a, ****}, V. A. Danilov^{a, *****},
M. L. Linderov^{a, *****}, and S. V. Zasyplin^{a, *****}

^aTogliatti State University, Togliatti, 445020 Russia

^bSt. Petersburg State University, Peterhof, St. Petersburg, 1998504 Russia

*e-mail: klevtsov11948@mail.ru

**e-mail: ruslan.valiev@ugatu.su

***e-mail: semenova-ip@mail.ru

****e-mail: inshtet@mail.ru

*****e-mail: V.Danilov@yandex.ru

*****e-mail: dartvi@gmail.com

*****e-mail: zvs181@mail.ru

Received August 13, 2018; revised November 19, 2018; accepted December 3, 2018

Abstract—The kinetics and mechanism of fatigue failure of the VT6 titanium alloy (composition, wt %: 5.95 V, 5.01 Al, 89.05 Ti) in the initial (hot-rolled) coarse-grained (CG) state and after equal-channel angular pressing (ECAP) in the ultrafine-grained state (UFG) are investigated. ECAP is performed using billets of the mentioned alloy 20 mm in diameter and 100 mm in length preliminarily subjected to homogenizing annealing. Then, quenching in water is performed from 960°C with holding for 1 h, tempering at 675°C for 4 h, and ECAP at 650°C (route B_c, $\phi = 120^\circ$, number of passes $n = 6$). The fine alloy structure after ECAP is investigated by transmission electron microscopy at an accelerating voltage of 200 kV. To determine alloy hardness, a Time Group TH 300 hardness meter is used. Static tensile tests are performed for round samples 5 mm in diameter using a Tinius Olsen H50KT universal testing machine. The extension velocity is 5 mm/min. Fatigue tests are performed using prismatic samples 10 mm in thickness at 20°C according to the three-point bending test using an Instron 8802 installation. It is shown that, under the same loading conditions, the fatigue life of alloy samples (the number of cycles before failure) in the initial CG state is higher than that of the alloy samples in the UFG state. It is shown that the number of cycles before fatigue-crack nucleation was at a level of 19–23% of the total sample longevity, regardless the alloy state. The straight-linear segment in kinetic diagrams of the alloy fatigue failure is approximated by the Paris equation. It is revealed that the propagation rate of the fatigue crack in the alloy with an UFG structure is somewhat higher than in the alloy with a CG structure. The microrelief of fatigue cleavages of the VT6 alloy both in the CG and UFG state can be characterized as scaly with fatigue grooves on the scale surface. A low-relief region 4–6 μm in length can be observed in the failure region of the samples with an UFG structure. The microrelief of the rupture region is pit, irrespective of the alloy state.

Keywords: fatigue failure, titanium alloy, failure kinetics and mechanism, coarse-grained (CG) state, ultrafine-grained (UFG) state, ECAP, Paris's equation

DOI: 10.3103/S1067821219030088

INTRODUCTION

The resistance of materials against fatigue failure is the most important characteristic of the constructive strength of materials. Therefore, numerous publications are devoted to investigating the fatigue strength and fatigue failure mechanism of ultrafine-grained (UFG) materials formed by severe plastic deformation (SPD) [1–14]. Strength increases and ductility decreases after the SPD, which usually leads to an increase in the fatigue limit of materials, but also a

decrease or insufficient increase in the fatigue strength in a low-cycle fatigue region [6, 7, 10, 15].

The authors in [7] and some other researchers [16, 17] showed that the UFG materials usually have higher crack propagation velocity in the time-independent mode when compared with coarse-grained (CG) alloy. The authors in [2, 7] associate the low strength of UFG materials in the low-cycle fatigue region with the smaller convolution of the propagating crack, which leads to a decrease in the roughness of cleavage surfaces [7] and with the relatively developed

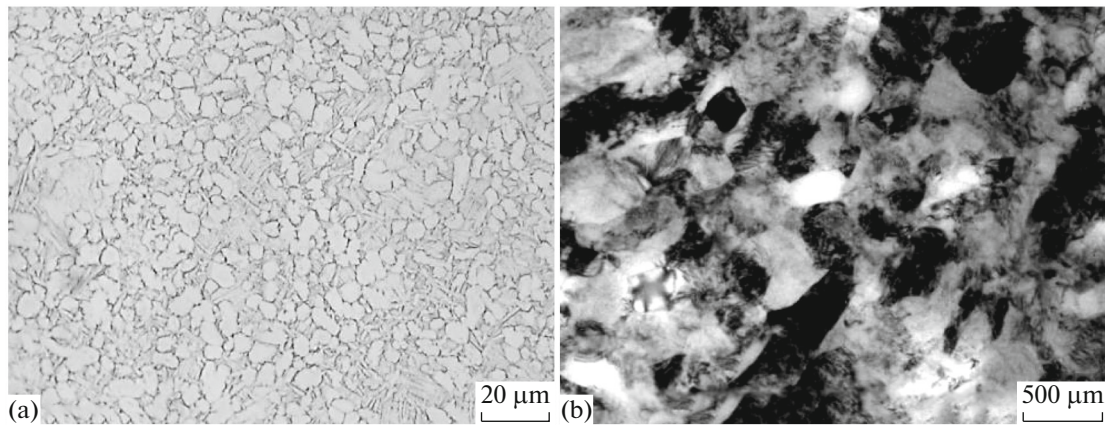


Fig. 1. Microstructure of the VT6 alloy (a) in the CG state (metallography) and (b) in the UFG state (TEM).

cyclic plastic deformation implemented near the crack vertex [2]. The low plasticity of UFG alloys unfavorably affects the low-cycle fatigue resistance, which strongly limits their practical application. Therefore, the most important direction of increasing the fatigue strength of UFG materials is the development of optimal SPD modes increasing their ductility [18–20].

This work is aimed at investigating the fatigue failure kinetics and mechanism of the VT6 titanium alloy with a UFG structure formed by equal-channel angular pressing (ECAP) in comparison with the initial coarse-grained (CG) state.

EXPERIMENTAL

The object of investigation was VT6 titanium alloy (composition, wt %: 5.95 V, 5.01 Al, and 89.05 Ti) in the initial CG state and in the UFG state after ECAP. The polymorphic transformation temperature in the alloy is $t_{pt} = 975 \pm 5^\circ\text{C}$. The initial state of the material is formed by hot rolling of the billets produced by VSMPO-AVISMA, Verkhnyaya Salda. The ECAP technology of the alloy was as follows. A billet 20 mm in diameter and 100 mm in length was subjected to homogenizing annealing. Then, quenching in water from 960°C with holding for 1 h, tempering at 675°C for 4 h, and ECAP at 650°C were performed (route B_c , $\varphi = 120^\circ$, number of passages $n = 6$) [18].

The alloy structure was studied using an optical and scanning electron (JEOL JSM-6390) microscopes (SEM). A fine alloy structure after ECAP is

investigated using a JEOL JEM 2100 transmission electron microscope (TEM) at an accelerating voltage of 200 kV. The alloy hardness tests were performed using a Time Group TH 300 hardness meter. Static tension of round samples 5 mm in diameter was performed using a Tinius Olsen H50KT universal testing machine with a velocity of 5 mm/min. Fatigue tests of prismatic samples 10 mm in thickness with a V-like ($r = 0.2$ mm) stress concentrator were performed at room temperature according to the three-point bending scheme using an Instron 8802 installation at $v = 10$ Hz, $R = 0.1$, and $\Delta P = 2000\text{--}4500$ N. The microfractographic analysis of cleavages was performed using a Sigma SEM (Carl Zeiss, Germany).

RESULTS AND DISCUSSION

Figure 1a shows the microstructure of the VT6 alloy in the initial state. In this case, the material in the initial billet has a mixed globular-platelet structure typical of hot-rolled rods and included the primary α phase in the form of equiaxial grains $15 \pm 5 \mu\text{m}$ and a region with a platelet ($\alpha + \beta$) structure. The volume fraction of a globular component of the α phase is about 65%.

The alloy thermal treatment and ECAP led to a decrease in size of primary grains of the α phase. The fraction of the UFG structure with an average grain/subgrain size of the α phase of 240 ± 60 nm was about 70% (Fig. 1b). Structural parameters of the VT6 alloy in the initial (CG) state and after ECAP in the UFG state are presented in Table 1.

Table 1. Structural parameters of the VT6 alloy

Alloy state	Average size of α and β grains/subgrains D_{av} , μm	Dislocation density $\rho \times 10^{15}$, m^{-2}	Fraction of the β phase, %
Initial (CG)	15 ± 5	0.19	15
After ECAP (UFG)	0.24 ± 0.60	1.28	8

It is seen from Table 2 that ECAP following the mentioned modes increases the hardness and strength characteristics of the VT6 alloy by a factor of approximately 1.2 but decreases ductility by a factor of 1.4.

Fatigue tests showed that, at the same load level (ΔP), the fatigue life (N_{tot} is the number of cycles before failure) of the samples with a stress concentrator in the CG state is higher than after ECAP (Table 3). The number of cycles before the nucleation of the fatigue crack (N_{nuc}) increases with an increase in sample fatigue life N_{tot} . Herewith, the value of N_{nuc} in the samples made of the CG alloy is higher than that of the UFG alloy, although in the percentage, irrespective of the alloy state, $N_{nuc} = 19\text{--}23\%$ of N_{tot} (Table 3).

Thus, the presence of a stress concentrator in the samples shortens the time before the fatigue-crack nucleation and, consequently, the total material fatigue life, to a larger extent in the UFG state when compared with the initial state.

The straight-linear segment in kinetic diagrams of the fatigue failure of the VT6 alloy depicted in Fig. 2 is approximated by the Paris equation:

$$dl/dN = C\Delta K^n,$$

where dl/dN is the propagation velocity of the fatigue crack, ΔK is the span of the stress intensity coefficient near the crack vertex, and C and n are coefficients.

The Paris equation for the CG alloy is depicted as $dl/dN = 7.6 \times 10^{-12} \Delta K^{3.6}$ and, for the UFG alloy, it has the form $dl/dN = 2.5 \times 10^{-11} \Delta K^{3.8}$.

Table 2. Mechanical properties of the VT6 alloy

Alloy state	HRC	σ_u , MPa	$\sigma_{0.2}$, MPa	δ , %
Initial (CG)	34	950 ± 20	849 ± 30	11.5 ± 1.5
After ECAP (UFG)	36	1090 ± 30	990 ± 40	8.3 ± 0.3

Table 3. Total fatigue life of the VT6 alloy samples before the failure and relative number of cycles before the fatigue crack nucleation in them

ΔP , N	N_{tot} , cycle		N_{nuc} , cycle/%	
	Initial	After ECAP	Initial	After ECAP
2000	—	1.07×10^5	—	$2.4 \times 10^4/22$
2500	1.18×10^5	5.76×10^4	$2.6 \times 10^4/23$	$1.15 \times 10^4/20$
3500	3.13×10^4	1.88×10^4	$6.5 \times 10^3/21$	$4.0 \times 10^3/21$
4500	1.59×10^4	—	$3.0 \times 10^3/19$	—

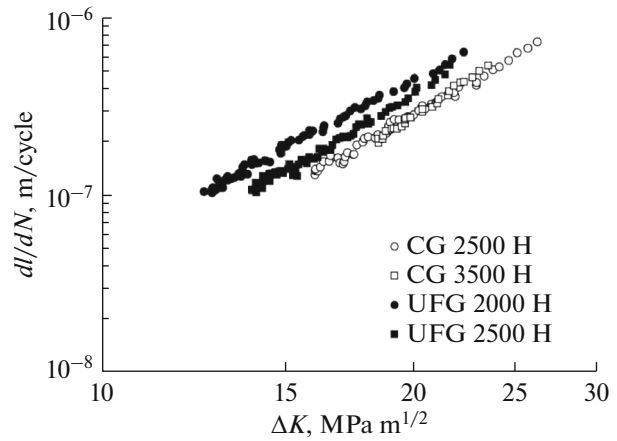


Fig. 2. Straight-linear segment of kinetic diagrams of the fatigue failure of the VT6 alloy in the initial state (empty signs) and after ECAP (filled signs).

It is seen from Fig. 2 that the fatigue-crack propagation velocity in the alloy with an UFG structure is somewhat higher than in the sample with a CG structure at the same ΔK . However, the values of coefficient n in the Paris equation are very close to one another (3.6 and 3.8), which points to the identical sensitivity of alloys to cyclic overloads [20].

Two zones are observed in formed cleavages, notably, the zone of the fatigue-crack development (l_f) and rupture zone [20, 21]. It is noteworthy that there is no clearly pronounced boundary between them (Fig. 3). The length of the l_f zone, depending on the load, is presented in Fig. 4. It is seen that values of l_f are larger for the alloy in the initial state than after ECAP for cleavages formed at the same value of ΔP .

Microfractographic investigations of fatigue cleavages of the VT6 alloy in the CG state showed that the elongation zone is absent in the failure region [21] and cylindrical cleavage facets are observed (Fig. 4a). The microrelief over the entire length of fatigue-crack development can be characterized as scaly (Figs. 4b, 4c).

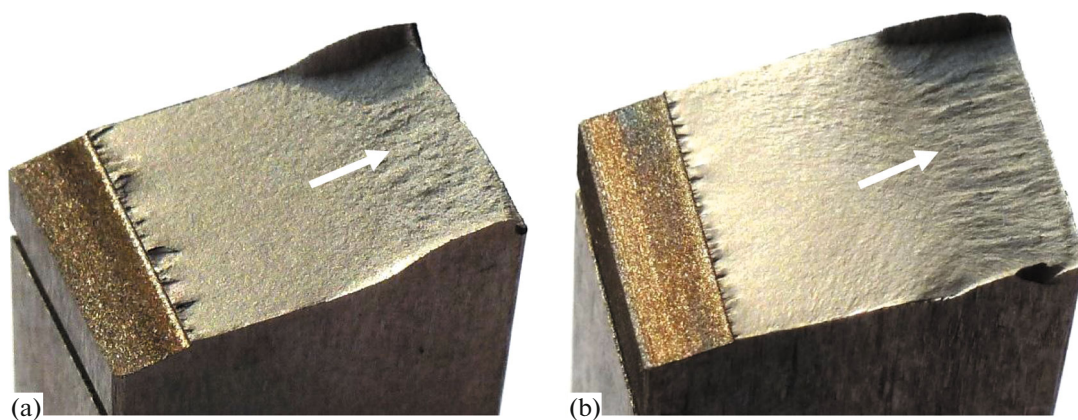


Fig. 3. Appearance of fatigue failures of the VT6 alloy (a) in the initial CG state and (b) after ECAP in the UFG state. (a) $\Delta P = 2500$ and (b) 2000 N. Arrows show the length of the crack fatigue development zone (l_f).

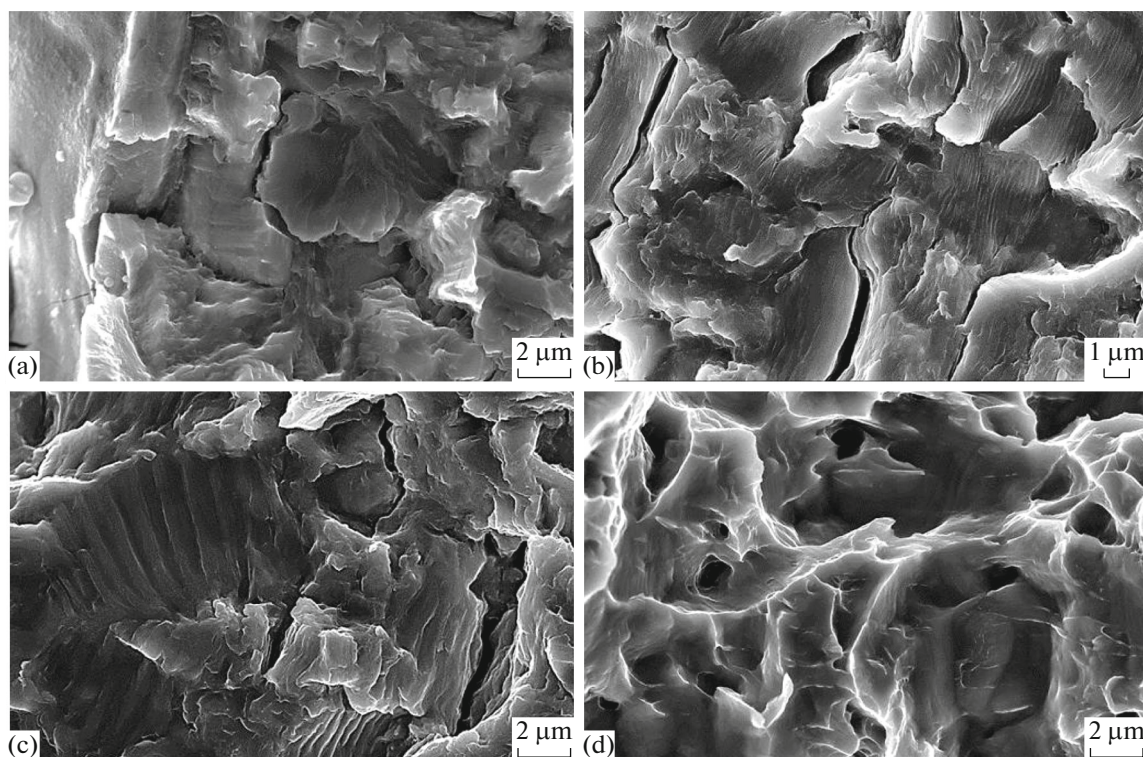


Fig. 4. Microrelief of the fatigue failure surface of the VT6 alloy in the CG state (magnification 5000 \times). (a) Microrelief in the failure region ($\Delta P = 2500$ N), (b) and (c) with a fatigue-crack length of (b) 3 mm and (c) 6 mm, and (d) in the rupture zone.

Table 4. Length of fatigue zone on the cleavage surfaces of the VT6 alloy samples in the initial state and after ECAP

$\Delta P, \text{ N}$	$l_f, \text{ mm}$	
	initial	after ECAP
2000	—	8.1
2500	8.6	7.1
3500	6.6	4.8
4500	5.5	—

Fatigue grooves are seen on the scale surface. The microrelief of the rupture zone consists of smooth nonuniform pits (Fig. 4d).

A microrelief region 4–6 μm in length can be observed in the failure region of fatigue cleavages of the alloy in the UFG state. Then the microrelief, similarly to the previous case, can be characterized as scaly with fatigue grooves on the scale surface (Figs. 5b, 5c). The rupture zone consists of very fine nonuniform smooth pits (Fig. 5d).

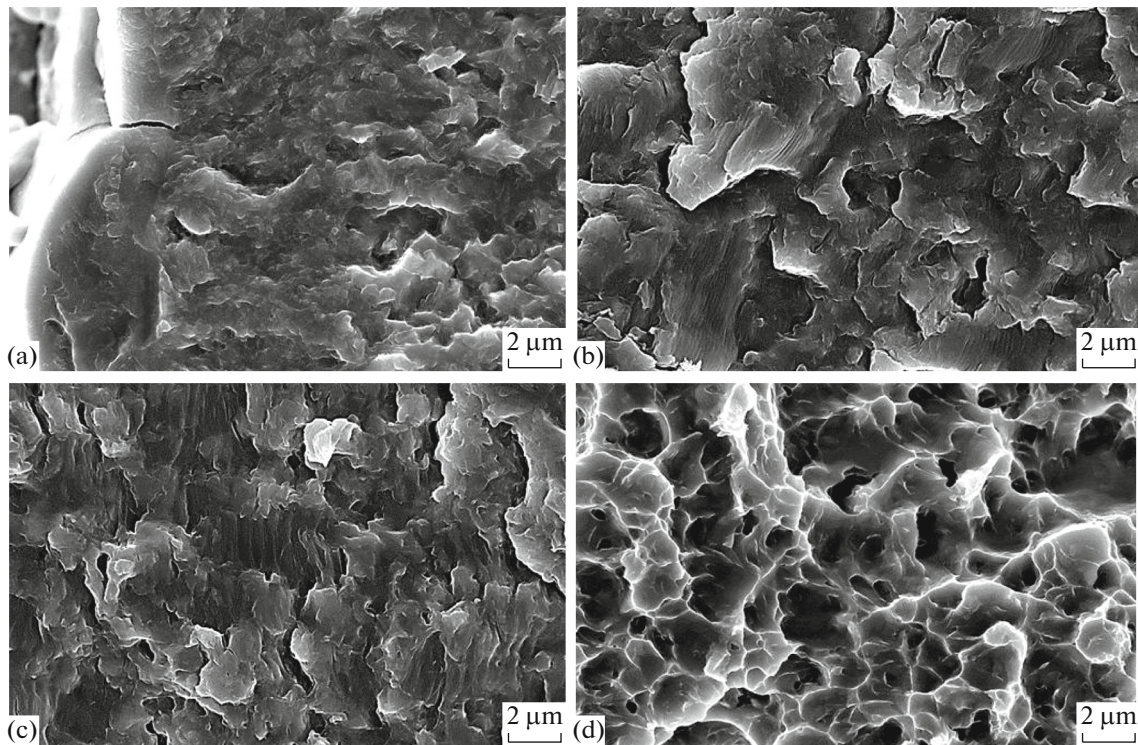


Fig. 5. Microrelief of the fatigue-failure surface of the VT6 alloy in the UFG state (magnification 5000 \times). (a) Microrelief in the failure region ($\Delta P = 2000$ N), (b) and (c) with a fatigue-crack length of (b) 3 mm and (c) 6 mm, and (d) in the rupture zone.

CONCLUSIONS

(i) The fatigue life of VT6 alloy samples with the stress concentrator is higher in the initial (CG) state than after ECAP in the UFG state under the same loading conditions. The number of cycles before the fatigue crack nucleation is at a level of 19–23% regardless of the alloy state.

(ii) The propagation rate of the fatigue crack in the alloy with an UFG structure is somewhat higher than in the CG material at the same ΔK in the Paris equation. However, values of coefficient n for both samples are almost indistinguishable.

(iii) The microrelief of fatigue cleavages of the VT6 alloy both in the CG and UFG state can be characterized as scaly with fatigue grooves on the scale surface. The microrelief of the rupture zone consists of smooth nonuniform pits, regardless of the alloy state.

FUNDING

This study was supported by the Russian Foundation for Basic Research, project no. 15-48-02119 r_po-vozh'e_a. RZV gratefully acknowledge the financial support from Saint Petersburg State University in the framework of Call 3 project (id 26130576).

CONFLICT OF INTERESTS

The authors claim that they have no conflict of interests.

REFERENCES

1. Chung, C.S., Kim, J.K., Kim, H.K., and Kim, W.J., Improvement of high-cycle fatigue life in a 6061 Al alloy produced by equal channel angular pressing, *Mater. Sci. Eng. A*, 2002, vol. 337, pp. 39–44.
2. Vinogradov, A., Nagasaki, S., Patland, V., Kitagawa, K., and Kawazoe, M., Fatigue properties of 5056 Al–Mg alloy produced by equal-channel angular pressing, *Nanostruct. Mater.*, 1999, vol. 11, pp. 925–934.
3. Furuya, Y., Matsuoka, S., Shimakura, S., Hanamura, T., and Torizuka, S., Effects of carbon and phosphorus addition on the fatigue properties of ultrafine-grained steels, *Scripta Mater.*, 2005, vol. 52, pp. 1163–1167.
4. Okayasu, M., Sato, K., Mizuno, M., Hwang, D.Y., and Shin, D.H., Fatigue properties of ultra-fine grained dual phase ferrite/martensite low carbon steel, *Int. J. Fatigue*, 2008, vol. 30, pp. 1358–1365.
5. Meyer, L.W., Sommer, K., Halle, T., and Hockauf, M., Crack growth in ultrafine grained AA6063 produced by equal-channel angular pressing, *J. Mater. Sci. Eng.*, 2008, vol. 43, pp. 7426–7431.
6. Meyer, L.W., Sommer, K., Halle, T., and Hockauf, M., Microstructure and mechanical properties affecting crack growth behaviour in AA6060 produced by equal-

- channel angular extrusion, *Mater. Sci. Forum*, 2008, vols. 584–586, pp. 815–820.
7. Estrin, Y. and Vinogradov, A., Fatigue behaviour of light alloys with ultrafine grain structure produced by severe plastic deformation: An overview, *Int. J. Fatigue*, 2010, vol. 32, pp. 898–907.
 8. Goto, M., Yamamoto, T., Kitamura, J., Iwamura, T., Han, S.Z., Ahn, J.-H., Kim, S., and Lee, J., Crack growth rate of inclined and deflected surface-cracks in round-bar specimens of copper processed by equal channel angular pressing under cyclic loading, *Eng. Fract. Mech.*, 2017, vol. 182, pp. 100–113.
 9. Estrin, Y. and Vinogradov, A., Extreme grain refinement by severe plastic deformation: A wealth of challenging science, *Acta Mater.*, 2013, vol. 61, pp. 782–817.
 10. Mughrabi, H., Hoppel, H.W., and Kautz, M., Fatigue and microstructure of ultrafine-grained metals produced by severe plastic deformation, *Scripta Mater.*, 2004, vol. 51, pp. 807–812.
 11. Wang, K., Tao, N.R., Liu, G., Lu, J., and Lu, K., Plastic strain-induced grain refinement at the nanometer scale in copper, *Acta Mater.*, 2006, vol. 54, pp. 5281–5291.
 12. Millett, P.C., Selvam, R.P., and Saxena, A., Stabilizing nanocrystalline materials with dopants, *Acta Mater.*, 2007, vol. 55, pp. 2329–2336.
 13. Khalaj, G., Khalaj, M.J., and Nazari, A., Microstructure and hot deformation behavior of AlMg6 alloy produced by equal-channel angular pressing, *Mater. Sci. Eng. A*, 2012, vol. 542, pp. 15–20.
 14. Skryabina, N.E., Pinyugzhanin, V.M., and Frushar, D., Features of the deformation texture formation in the AZ31 magnesium alloy during equal-channel angular pressing, *Perspekt. Mater.*, 2013, no. 1, pp. 33–42.
 15. Islamgaliev, R.K., Nesterov, K.M., Khafizova, E.D., Ganeev, A.V., Golubovskii, E.R., and Volkov, M.E., Strength and fatigue of the AK4-1 ultrafine-grained aluminum alloy, *Vestn. UGATU*, 2012, no. 8, pp. 104–109.
 16. Valiev, R.Z., Semenova, I.P., Latysh, V.V., Shcherbakov, A.V., and Yakushina, E.B., Nanostructural titanium for biomedical applications: new developments and prospects of commercialization, *Ross. Nanotekhnol.*, 2008, nos. 9–10, pp. 80–89.
 17. Klevtsov, G.V., Valiev, R.Z., Botvina, L.R., Klevtsova, N.A., Semenova, I.P., Kashapov, M.R., Fesenyuk, M.V., and Soldatenkov, A.P., Kinetics of fatigue fracture of titanium in a submicrocrystalline state, *Vestn. OGU*, 2012, no. 9, pp. 123–125.
 18. Valiev, R.Z., Zhilyaev, A.P., and Langdon, T.G., *Bulk Nanostructured Materials: Fundamentals and Applications*, TMS-Wiley, 2014.
 19. Valiev, R.Z., Raab, G.I., Gunderov, D.V., Semenova, I.P., and Murashkin, M.Yu., Development of methods of intense plastic deformation to form bulk nanostructured materials with unique mechanical properties, *Nanotekhnika*, 2006, no. 2, pp. 32–42.
 20. Klevtsov, G.V., Bobruk, E.V., Semenova, I.P., Klevtsova, N.A., and Valiev, R.Z., *Prochnost' i mekhanizmy razrusheniya ob'emnykh nanostrukturirovannykh metallicheskih materialov: Uchebnoe posobie* (Durability and Destruction Mechanisms of Bulk Nanostructured Metal Materials: Textbook), Ufa: Ufimsk. Gos. Aviats. Tekh. Univ., 2016.
 21. Klevtsov, G.V., Botvina, L.R., Klevtsova, N.A., and Limar', L.V., *Fraktodiagnostika razrusheniya metallicheskih materialov i konstruksii* (Fractography of Fracture of Metallic Materials and Constructions), Moscow: MISiS, 2007.

Translated by N. Korovin